

Open circuit fault detection in PWM voltage source inverter for PMSM drive system

Anuttar J. Shende

Department of Electrical Engineering, PESMCOE, Pune, Maharashtra, India

Abstract— In this paper, a simple and low-cost open-circuit fault detection and **identification method** for a pulse-width modulated (PWM) voltage-source inverter (VSI) employing a permanent magnet synchronous motor is proposed. An open-circuit fault of a power switch in the PWM VSI changes the corresponding terminal voltage and introduces the voltage distortions to each phase voltage. The proposed open-circuit fault diagnosis method employs the model reference adaptive system techniques and requires no additional sensors or electrical devices to detect the fault condition and identify the faulty switch. The proposed method has the features of fast diagnosis time, simple structure, and being easily inserted to the existing control algorithms as a subroutine without major modifications. The simulations and experiments are carried out and the results show the effectiveness of the proposed method.

Key Words : Fault detection, fault diagnosis, fault identification, model reference adaptive system (MRAS), open-circuit fault, pulse-width modulated voltage-source inverter (PWM VSI)..

1 INTRODUCTION

The permanent magnet synchronous motor (PMSM) is increasingly used in powered wheelchairs, electric vehicles, aerospace, medical and military applications, and nuclear power plants due to its advantages such as high power density, torque to inertia ratio, efficiency, and simple control [1].

In these applications, because an accident or fault can result in huge damages to the human life and environments, the reliability of the machine drives is one of the most important factors to guarantee the safe, continuous and high performance operation under even some accidents or faults. Generally, when an accident or fault occurs, the drive system has to be stopped for emergency or non programmed maintenance schedule. Due to the high cost of unexpected maintenance, the development of a reliable system is the area of interest. A control system with minimum or zero effects from the faults is called a "fault-tolerant control system," and it

performs the following three tasks [2]: 1) fault detection; 2) fault identification; and 3) remedial actions. The fault detection is the process to determine whether the system is healthy or not. The fault identification is performed after the fault detection to identify the location, type, and nature of the fault. Finally, the remedial actions, also known as fault isolation, are the process to remove the faulty devices and re configure the system for a safe and continuous operation. Among these three tasks, the fault detection and fault identification are considered as a prime process for the practical implementation and are often called as a "fault diagnosis."

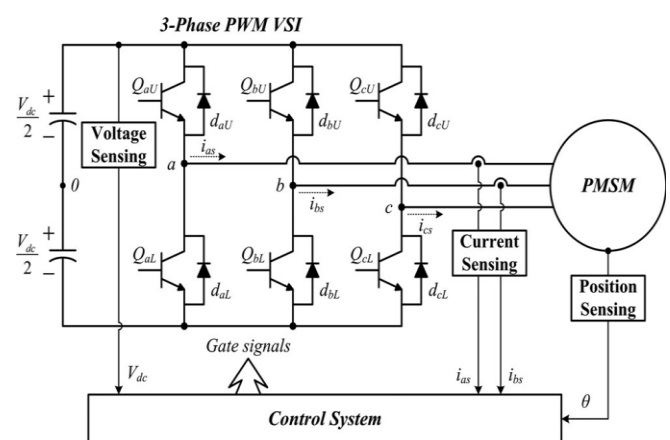


Fig -1: Basic block diagram of PWM VSI for PMSM drive system.

This fault-tolerant control strategy [1], [2] can be activated either in the case of the normal mode of operation or in the case of the faulty "open-delta" mode of operation. In other words, the compensation algorithm is continuously running during the healthy operation without any detectable negative impact on the system performance. However, the compensation algorithm will have a significant impact on the system performance under the faulty condition in diminishing or alleviating the undesirable effects of the fault and, consequently, enhancing the robustness of the system. Therefore, no activation algorithm for the introduced fault-tolerant strategy is required. Moreover, this fault-mitigation

strategy is insensitive to the variation in motor parameters and it is applicable to both open-loop scalar “volts per-hertz” (see [1]) and vector-control motor-drive systems as will be shown in this paper.

On the other hand, the power converter failures can be a critical factor to the overall drive system and cause system shutdowns; therefore, these require a high cost of unexpected maintenance. It is estimated that about 38% of all the failures are found in the power converter [8] and the most of faults are occurred to the power switches [9]. In response to a control algorithm, a voltage command is generated, and the VSI synthesizes this voltage command using the power switches, i.e., insulated-gate bi polar transistor (IGBT) and MOSFET, with the techniques such as the sinusoidal PWM (SPWM) or space vector PWM (SVPWM). There could be a quite high chance of failure in the switching devices due to the high electrical and thermal stresses [10]. The failure of switching devices can take place in the form of short circuit or open circuit. The short circuit fault may occur due to an improper gate signal so that both power switches in a leg of the VSI are turned ON. This results in a short circuit of the capacitor in the dc link that blows out the other components particularly switching devices. Therefore, the short-circuit fault is one of them fatal accidents and the most important thing in the drive system is to minimize the time between short-circuit fault initiation and appropriate reaction.

Consequently, the control circuits of the switching devices are designed to have a fast fault diagnosis characteristic to prevent the abnormal over current and mostly the hardware-based protection schemes are employed. The open-circuit fault, on the other hand, is often overlooked since it has the characteristic of slow response and less danger to the whole drive system compared with the short-circuit fault. The open-circuit fault may result from the disconnection of a wire from the switching devices due to a thermic cycling or a gate driver failure. The open-circuit fault leads to the current imbalance in both the faulty and healthy phases and results in the pulsating currents and torques, which highly degrades the driving performances. The open-circuit fault is not generally harmful to the machine drives and does not cause system shutdowns, but could lead to the secondary faults at the other components [3]. The open circuit fault is one of the general faults and can be frequently taken place in the drive system, though, and the literature has much concerned about the fault.

This paper proposes a simple and low-cost open-circuit fault diagnosis algorithm in the PWM VSI for PMSM. Such technique requires no additional sensors and is based on the analytical model of the PWM VSI. The proposed fault diagnosis method has the fast, simple and low-cost characteristics and can be easily embedded in the existing PMSM drive system as a subroutine without major **modifications** [4]. This proposed method is implemented in a digital manner using a MCUTMS320F28335 from Texas Instruments, Incorporated. The simulation and experimental results show the validity of the proposed

diagnosis method.

2 Two-Phase Operation Of Delta-Connected Machines

The two-phase operation of an inverter-fed induction motor with delta-connected stator phase windings has **two possible network configuration scenarios**. The first scenario is that one of the power lines connecting the supply voltage to the motor is disconnected. This might be due to a blown fuse, an accidental rupture in the cable connecting the drive to the motor, or a faulty switch or failure of the gate drive circuit of a switch. In this case, a **motor’s phase currents will not be independent of each other**, hence losing two degrees of freedom, and the machine will operate as a single-phase machine. The second scenario is that one of the phases in the stator winding is disconnected as shown in Fig. 1. This might be due to one of the reasons mentioned earlier in Section I. It should be noted that the analysis and the topology presented in this paper are centered on providing an acceptable motor performance while the machine is running under a faulty condition that resembles the second scenario which will be referred to throughout the **remainder of this paper as a “two-phase open-delta mode of operation.”**

As mentioned earlier, it is presumed that the motor windings are connected to the supply voltage. However, one of the motor phases was disconnected due to an internal fault in the windings as depicted in Fig. 1. Therefore, the relationship between the motor terminal (line) currents, $i_A(t)$, $i_B(t)$, $i_C(t)$ and phase currents $i_a(t)$, $i_b(t)$, $i_c(t)$ can be expressed as follows:

$$\begin{pmatrix} i_A(t) \\ i_B(t) \\ i_C(t) \end{pmatrix} = \begin{pmatrix} -1 & 1 & 0 \\ 0 & -1 & 1 \\ 1 & 0 & -1 \end{pmatrix} \begin{pmatrix} i_a(t) \\ i_b(t) \\ i_c(t)=0 \end{pmatrix} \quad (1)$$

In order to clarify this discussion, let us assume that the line currents are set by the inverter to be equal to $i_C(t)=i_a(t)= I_m \cos(\omega t)$ and $i_B(t) = -i_b(t) = I_m \cos(\omega t - \psi)$ while phase c is isolated. This means that the resultant MMF of the stator can be expressed as follows:

$$F_s(t) = N_s \{ \cos(\theta) i_a + \cos(\theta - 2\pi/3) i_b \} \quad (2)$$

And

$$F_s(t) = F_+ s(t) + F_- s(t) = (N_s I_m) / 2 \{ \cos(\theta - \omega t) + \cos(\theta + \omega t) - \cos(\theta - \omega t - 2\pi/3 + \psi) - \cos(\theta + \omega t - 2\pi/3 - \psi) \} \quad (3)$$

where I_m is the peak value of the phase current and N_s is the effective number of stator winding turns per phase.

From (3), the induced rotor MMF can be expressed as

$$F_r(t) = F_+ r(t) + F_- r(t) = (N_r I_r m) / 2 \{ \cos(\theta - \omega t + \delta) \}$$

$$+ \cos(\theta + \omega t + \delta) - \cos(\theta - \omega t - 2\pi/3 + \psi + \delta) - \cos(\theta + \omega t - 2\pi/3 - \psi + \delta) \quad (4)$$

where δ is known as the angle between the stator and the rotor MMFs which is also known as the power angle, and it is equal to π at no-load condition, and ψ is a controllable phase shift. The negative sequence of the MMF component of the stator can be set to zero by controlling the stator line currents such that $\psi = 4\pi/3$. In this case, the resultant stator MMF is expressed as follows:

$$F_s(t) = F + s(t) = N_s I_m \sqrt{2} \{ \cos(\theta - \omega t) - \cos(\theta - \omega t + 2\pi/3) \} \quad (5)$$

Or

$$F_s(t) = F + s(t) = \sqrt{3} (N_s I_m) / 2 \{ \cos(\theta - \omega t - \pi/3) \}. \quad (6)$$

Also, the induced rotor MMF component in this case can be given by

$$F_r(t) = (N_r I_r m) / 2 \{ \cos(\theta - \omega t + \delta) - \cos(\theta - \omega t + 2\pi/3 + \delta) \} \quad (7)$$

or

$$F_r(t) = F_r(t) = \sqrt{3} (N_r I_r m) / 2 \{ \cos(\theta - \omega t - \pi/3 + \delta) \}. \quad (8)$$

Inspection of (6) shows that the magnitude of the remaining two active phase currents should be increased by a factor of $\sqrt{3}$ in order to maintain the same amplitude of the stator MMF, $\{(3/2)(N_s I_m)\}$, under healthy conditions. This means that the line currents are reset to $i_C(t) = \sqrt{3} I_m \cos(\omega t)$ and $i_B(t) = \sqrt{3} I_m \cos(\omega t - 4\pi/3)$. However, if the motor phase currents in the remaining two active phases are limited to the rated phase value current I_m , the output power will be limited to $(1/\sqrt{3})$ of the rated power. In other words, in delta-connected machines, the line current is equal to $\sqrt{3}$ of the phase current in the windings, $I_L = \sqrt{3} I_{ph}$. Consequently, in either case, delta or open-delta, the fundamental component of the converter current does not change. On the other hand, since the motor phase current is equal to them or line current in the case of open-delta mode of operation, the current in them or phase windings will increase in the case of open-delta mode of operation by a factor of $\sqrt{3}$ as compared to healthy delta-connected machines. Hence, this will require power derating by a factor of $1/\sqrt{3}$. This fact can be also verified from the MMF expression under faulty open-delta mode of operation [see(6)] as compared to the MMF expression under normal mode of operation.

3. ANALYSIS OF THE OPEN-CIRCUIT FAULT IN THE PWM VSI

Fig.2 shows the basic configuration of phase A leg of a three phase PWM VSI. When the system is under the normal condition as can be seen in Fig. 2(a), the terminal voltage of phase A, v_{a0} , is determined by the phase current i_{as} and the switching function S_a of Q_{aU} and Q_{aL} . If the switching function is 1, which means that Q_{aU} is turned ON and Q_{aL} is turned OFF, the terminal voltage of

phase A is equal to $V_{dc}/2$, where V_{dc} is the dc-link voltage. If the switching function is 0, which means that Q_{aU} is turned OFF and Q_{aL} is turned ON, $v_{a0} = -V_{dc}/2$. The possible terminal voltages according to the switching function and the direction of phase current under the normal condition are represented in Table I. Unlike the normal condition, however, an open-circuit fault in the upper switch Q_{aU} results in changing the corresponding terminal voltage when the phase current i_{as} is positive and the switching function S_a is 1, since the upper switch Q_{aU} is not working properly. In this case, the terminal voltage of phase A is not equal to $V_{dc}/2$, but equal to $-V_{dc}/2$.

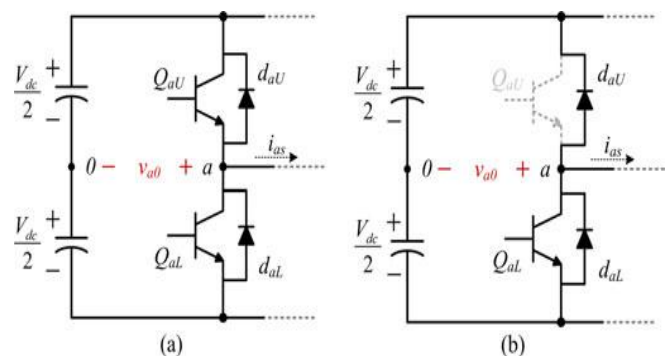


Fig. 2. Basic configuration of phase A leg of a three-phase PWM VSI. (a) Normal condition. (b) Open-circuit fault in the upper switch Q_{aU} .

The equivalent circuit after the open-circuit fault occurrence to the upper switch Q_{aU} is shown in Fig. 2(b), and the corresponding terminal voltages are represented in Table II.

TABLE I

TERMINAL VOLTAGES OF PHASE A UNDER THE NORMAL CONDITION

	$S_a = 1$	$S_a = 0$
$i_{La} \geq 0$	$v_{a0} = \frac{V_{dc}}{2}$	$v_{a0} = -\frac{V_{dc}}{2}$
$i_{La} < 0$	$v_{a0} = \frac{V_{dc}}{2}$	$v_{a0} = -\frac{V_{dc}}{2}$

TABLE II
TERMINAL VOLTAGES OF PHASE A UNDER THE OPEN-CIRCUIT FAULT CONDITION

	$S_a = 1$	$S_a = 0$
$i_{La} \geq 0$	$v_{a0} = -\frac{V_{dc}}{2}$	$v_{a0} = \frac{V_{dc}}{2}$
$i_{La} < 0$	$v_{a0} = \frac{V_{dc}}{2}$	$v_{a0} = -\frac{V_{dc}}{2}$

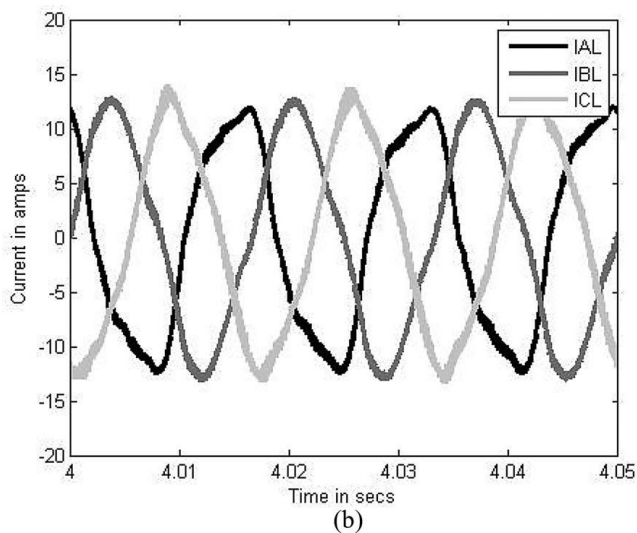
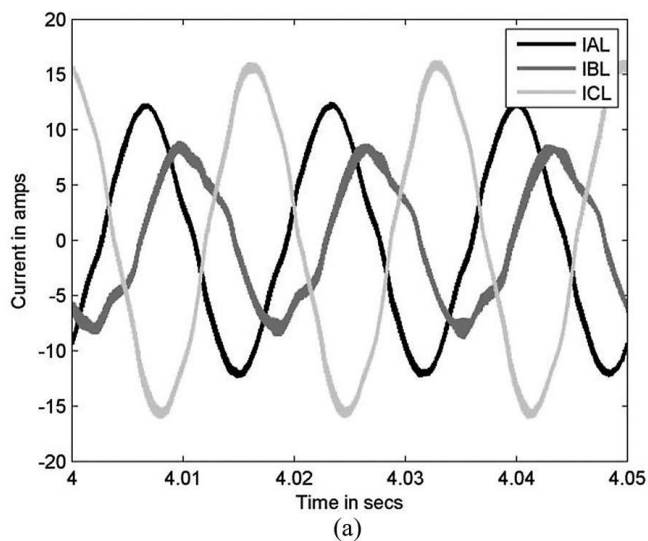
From the aforementioned analysis, it is obvious that the phase voltages may have the voltage deviations in the steady state after the fault occurrence from the normal condition. Based on this fact, the proposed fault diagnosis method indirectly observes these voltage deviations using the analytical model of the PWM VSI and the fault diagnosis can be achieved.

4. ANALYSIS OF SIMULATION AND EXPERIMENTAL RESULTS

In order to examine and verify the previously introduced fault mitigation strategy, several simulation and experimental results are explored in this section. The case-study motor is a 5-hp six pole induction motor, which was designed such that it can be configured either as a six-phase or as three-phase induction motor, with the stator connected either as Yordelta. The stator consists of 36 stator slots and 45 rotor bars with closed slots. These design particular simplified the existence of the third, fifth, and seventh harmonics in the phase currents, and, consequently, the fifth and seventh harmonics in the line currents. The total harmonic distortion (THD) for the line currents is 1.6% and the THD of the phase currents is 3%.

Meanwhile, the motor-drive system was experimentally tested at several operating conditions. The power structure of a 10-hp commercial drive was interfaced to a DSP board (EZDSP F2812) in which the DSP chip (TMS320F2812) is the main processor that hosted the algorithms introduced earlier in this paper. The currents' sampling rate was set to 5 kHz. This new control

algorithm was executed through an "interrupt service routine" which was periodically called every 200 μ s. The carrier/switching frequency was set to 5 kHz. The effectiveness of this introduced controller for the case of open-loop motor-drive system can be verified through comparing the unbalanced line-current waveforms for the case of two-phase open-delta operation while the machine is operating at half-load condition at 60-Hz inverter output frequency. These results were obtained when the newly introduced controller was deactivated, and the balanced line-current waveforms for the case of two- The effectiveness of this introduced controller for the case of open-loop motor-drive system can be verified through comparing the unbalanced line-current waveforms for the case of two-phase open-delta operation while the machine is operating at half-load condition at 60-Hz inverter output frequency. These results were obtained when the newly introduced controller was deactivated, and the balanced line-current waveforms for the case of two- phase



open-delta operation, when this newly introduced controller was activated. The corresponding experimental results at the same operating conditions are depicted in. It can be observed that the compensation strategy was able to minimize the negative-sequence component of the fundamental frequency in the motor line currents. It should be pointed out that this controller compensates only for the unbalance in the fundamental components of the motor currents but not for the harmonics in the motor winding currents.

B. Experimental Result

In order to confirm the feasibility of the fault diagnosis algorithm, the experiments have been realized under the same conditions as the simulations. The parameters related to the test motor and PWM VSI are represented in Tables VI and VII, respectively. The three-phase PWM VSI is composed of six IGBTs, FGH40N60SFD from Fairchild, Corp. The switching frequency of the PWM VSI

is 11 kHz. All the control laws proposed in this paper have been realized by using a single MCU TMS320F28335 from Texas Instruments, Incorporated. The sampling rate of phase currents is identical to the switching frequency. The open-circuit fault condition is made by introducing no gate drive signal to the IGBT.

TABLE VI
SPECIFICATIONS OF THE TEST PMSM

Rated Power	750 [W]	# of poles	8
Rated Torque	2.4 [Nm]	Rated Speed	3000 [r/min]
Phase Resistance	0.49 [Ω]	Rated Current	6.0 [A]
Linkage Flux	0.0667 [Wb]	Phase Inductance	6.9 [mH]

TABLE VII
SPECIFICATIONS OF THE PWM VSI

DC-link Voltage	300 [V]	Switching Frequency	11 [kHz]
Dead-time	2.8 [μ sec]	Switching Device	IGBT
Turn-on Time [†]	25 [nsec]	Turn-off Time [†]	115 [nsec]
Saturation Voltage [†]	2.5 [V]	Forward Voltage [†]	1.95 [V]

[†]Fairchild datasheet (FGH40N60SFD).

Fig. 3(a) shows the experimental results for the process of the fault diagnosis algorithm.

As can be seen in this figure, when all of the switching devices are under the normal condition, the observed voltage distortion is nearly zero. However, there is a significant difference after the fault occurrence to the upper switch QaU , and the error signal is generated. When the error detection time t_e continuously elapses and exceeds beyond the fault detection time $T_{f\ ault}$ defined, the fault detection flag $FlagD$ changes from low to high. Fig.3(b) shows the fault identification flag $FlagI$ composed of three flags $FlagA$, $FlagB$, and $FlagC$ that identify the faulty switch. In this case, "100" means that the open-circuit fault has been occurred to the upper switch QaU . Fig.4 shows the similar experimental results in the case of the rated speed, 3000 r/min.

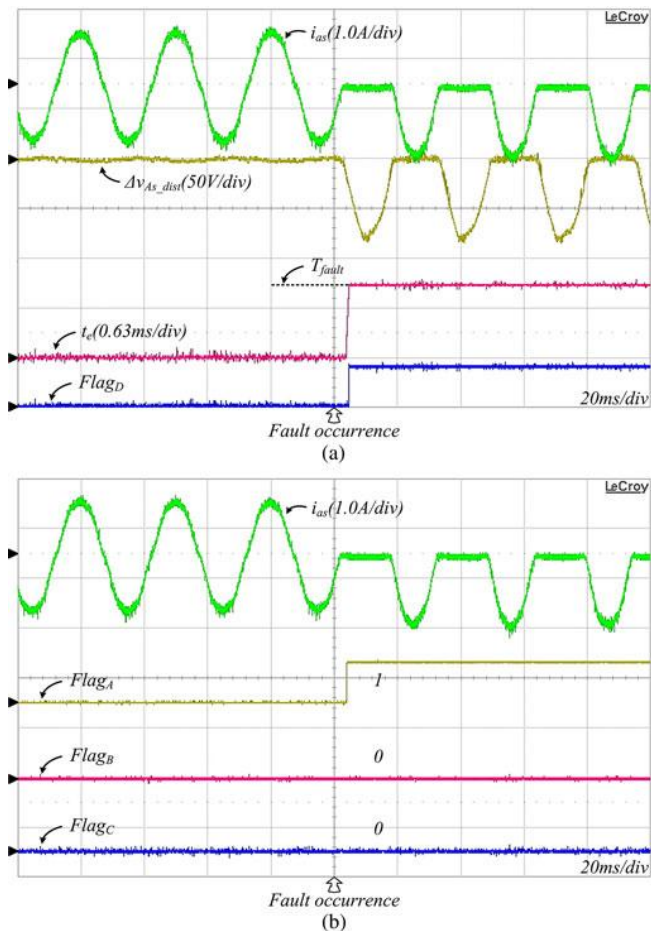


Fig. 3. Experimental results of the fault diagnosis when the open-circuit fault occurs to the upper switch QaU (500 r/min). (a) Process of the proposed fault diagnosis algorithm. (b) Fault identification.

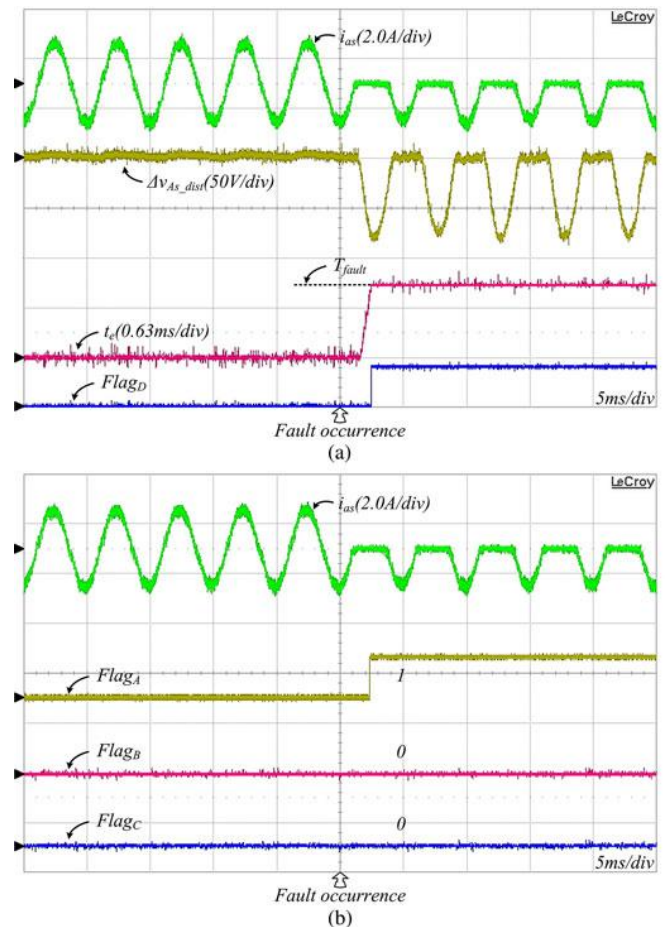


Fig. 4. Experimental results of the fault diagnosis when the open-circuit fault occurs to the upper switch QaU (3000 r/min). (a) Process of the proposed fault diagnosis algorithm. (b) Fault identification.

5. CONCLUSION

The fault detection and identification is becoming more and more important for industrial applications. Therefore, it is increasingly required to improve the fault diagnosis capabilities. In this paper, a simple and low-cost open-circuit fault detection and identification method is presented. The proposed fault diagnosis is achieved by the simple voltage distortion observer. Once the voltage distortions are estimated, these are compared with the threshold value to determine the fault condition. When the open-circuit fault occurs, the observed voltage distortions are bigger than the threshold value. By comparing these two values, the fault condition is decided. Also, the fault identification is achieved by using the observed voltage distortions, since the voltage distortions are different according to the faulty switch. The fault-tolerant control strategy presented in an earlier publication for the case of open-loop motor-drive system is extended for the case of vector-control motor-drive system. The performance of

the introduced fault-mitigation strategy was examined and compared under both control techniques. It was shown that the introduced fault-mitigation strategy is able to alleviate the output torque pulsations and the line current while running under two-phase open-delta mode of operation for the case of vector-control motor-drive system and for the case of open-loop motor-drive system. However, the existence of the CCW current controllers in the vector control leads to the fact that it is able to dampen/alleviate the unbalance in the motor line current faster with less transient peak magnitude while transferring from balanced three-phase mode of operation to two-phase mode of operation especially at lower operating speed. The introduced technique takes advantage of the additional degree of freedom of the stator phase currents in the two remaining active phases of this configuration.

REFERENCES

- [1] A. Sayed-Ahmed and N. A. O. Demerdash, "Fault-tolerant operation of delta-connected scalar- and vector-controlled AC motor drives," *IEEE Trans. Power Electron.*, vol. 27, no. 6, pp. 3041–3049, Jun. 2012
- [2] B. K. Lee, T. H. Kim, and M. Ehasani, "On the feasibility of four-switch three-phase BLDC motor drives for low cost commercial applications: Topology and control," *IEEE Trans. Power Electron.*, vol. 18, no. 1, pp. 164–172, Jan. 2003.
- [3] D. Diallo, M. E. H. Benbouzid, D. Hamad, and X. Pierre, "Fault detection and diagnosis in an induction machine drive: A pattern recognition approach based on concordia stator mean current vector," *IEEE Trans. Energy Convers.*, vol. 20, no. 3, pp. 512–519, Sep. 2005.
- [4] H. Berriri, M. W. Naouar, and I. Slama-Belkhodja, "Easy and fast sensor fault detection and isolation algorithm for electrical drives," *IEEE Trans. Power Electron.*, vol. 27, no. 2, pp. 490–499, Feb. 2012.
- [5] J. O. Estima and A. J. M. Cardoso, "A new algorithm for real-time multiple open-circuit fault diagnosis in voltage source inverters," *IEEE Trans. Ind. Electron.*, vol. 47, no. 6, pp. 2487–2494, Nov./Dec. 2011.
- [6] K. Rothenhagen and F. W. Fuchs, "Current sensor fault detection, isolation, and reconfiguration for doubly fed induction generator," *IEEE Trans. Ind. Electron.*, vol. 56, no. 10, pp. 4239–4245, Oct. 2009.
- [7] R. Peugeot, S. Courtine, and J. P. Rognon, "Fault detection and isolation on a PWM inverter by knowledge-based model," *IEEE Trans. Ind. Appl.*, vol. 34, no. 6, pp. 1318–1326, Nov./Dec. 1998
- [8] S. Karimi, A. Gaillard, P. Poure, and S. Saadate, "FPGA-based realtime power converter failure diagnosis for wind energy conversion systems," *IEEE Trans. Ind. Electron.*, vol. 55, no. 12, pp. 4299–4308, Dec. 2008.
- [9] S. Khomfoi and L. M. Tolbert, "Fault diagnosis and reconfiguration for multilevel inverter drive using ai-

based techniques," *IEEE Trans. Ind. Electron.*, vol. 54, no. 6, pp. 2954–2968, Dec. 2007.

[10] U. M. Choi, H. G. Jeong, K. B. Lee, and F. Blaabjerg, "Method for detecting an open switch fault in a grid connected NPC inverter system," *IEEE Trans. Ind. Electron.*, vol. 27, no. 6, pp. 2726–2739, Jun. 2012.

[11] W. Sleszynski, J. Nieznanski, and A. Cichowski, "Open-transistor fault diagnostics in voltage-source inverters by analyzing the load currents," *IEEE Trans. Ind. Electron.*, vol. 56, no. 11, pp. 4681–4688, Nov. 2009.